Journal of Electrochemistry

Volume 23
Issue 5 *Special Issue on Supercapacitors*

2017-10-28

Attempts to Improve the Energy Capacity of Capacitive Electrochemical Energy Storage Devices

Lin-po YU

Z. CHEN George
Department of Chemical and Environmental Engineering, and Centre for Sustainable Energy Technologies, Faculty of Science and Engineering, University of Nottingham Ningbo China, Ningbo 315100, Zhejiang, China;Department of Chemical and Environmental Engineering, Faculty of Engineering, University of Nottingham, Nottingham NG7 2RD, UK;, george.chen@nottingham.edu.cn

Recommended Citation

Lin-po YU, Z. CHEN George. Attempts to Improve the Energy Capacity of Capacitive Electrochemical Energy Storage Devices[J]. *Journal of Electrochemistry*, 2017 , 23(5): 533-547.
DOI: 10.13208/j.electrochem.170347
Available at: https://jelectrochem.xmu.edu.cn/journal/vol23/iss5/4

This Review is brought to you for free and open access by Journal of Electrochemistry. It has been accepted for inclusion in Journal of Electrochemistry by an authorized editor of Journal of Electrochemistry.

DOI: 10.13208/j.electrochem.170347 **Artical ID**:1006-3471(2017)05-0533-15
Cite this: *J. Electrochem.* **2017**, *23*(5): 533-547 **Http**://electrochem.xmu.edu.cn

Attempts to Improve the Energy Capacity of Capacitive Electrochemical Energy Storage Devices

YU Lin-po[1], George Z. CHEN[1,2*]

(1. *Department of Chemical and Environmental Engineering, and Centre for Sustainable Energy Technologies, Faculty of Science and Engineering, University of Nottingham Ningbo China, Ningbo* 315100, *Zhejiang, China;* 2. *Department of Chemical and Environmental Engineering, Faculty of Engineering, University of Nottingham, Nottingham NG7 2RD, UK*)

Abstract: This article reviews selected literatures from the authors' research group on the development of capacitive electrochemical energy storage (EES) devices, focusing on supercapacitors and supercapatteries at both the electrode material level and device level. Electronically conducting polymers (ECPs) and transition metal oxides (TMOs) composited with carbon nanotubes (CNTs) were found to be able to improve the capacitance performance as capacitive faradaic storage electrode. Carbon materials, like activated carbon (Act-C) and carbon black, were used to fabricate non-faradaic capacitive storage electrode. It was found that the electrode capacitance balance can effectively extend the maximum charging voltage (MCV) of the supercapacitor, and hence, to enhance the energy capacity of this capacitive EES device. The MCV of this kind of device can also be multiplied by bipolarly stacking the supercapacitors to meet the high voltage demand from the power device. Supercapatteries that take advantages of both capacitive and faradaic charge storage mechanisms have been proposed and demonstrated to achieve the high power capability of supercapacitors and the large storage capacity of batteries.

Key words: supercapacitor; supercapattery; pseudocapacitive; carbon nanotubes; activated carbons
CLC Number: O646 **Document Code**: A

Sustainable energy technologies have been attracting more and more global attention due to the foreseeable exhaustion of fossil reserves and the non-negligible negative environmental impact of CO_2 emission accompanied with the consumption of fossil fuels. Thanks to the gradually reducing costs of harvesting renewable energy sources such as sunlight, wind, and tide, some of these sustainable energy technologies like promoting solar and geothermal energies are either economically competitive or close to being so[1]. The harvested renewable energies demand efficient and economical energy storage technologies in competition with the traditional non-renewable options[2]. Electrochemical energy storage (EES) devices, including rechargeable batteries and supercapacitors (also known as electrochemical capacitors), can store charges in a fast and efficient way, and hence help harvest and convert renewable energy to a usable form. A great of global efforts have been made to develop the EES technologies and relevant materials to meet the challenges of sustainable energy supply[3-9]. The past two decades have witnessed the significant progresses on both rechargeable batteries and supercapacitors researches, while each alone still cannot go beyond its limitation, like the poor power capability for rechargeable batteries based on electrochemical reactions and the limited energy capacity for supercapacitors based on capacitance. Recently, researchers published the innovative proposal and preliminary demonstration of serval hybrid devices that combines the rechargeable battery and supercapacitor characteristics into one device[10]. We can call the device su-

Received: 2017-03-06, Revised: 2017-07-07 *Corresponding author, Tel: (86-574)88180000-9696, E-mail: george.chen@nottingham.edu.cn

percapattery because it demonstrates a capacitive behaviour and possesses a greater energy capacity than a supercapacitor[11-13]. Supercapattery can be regarded as the next generation of capacitive EES devices after supercapacitors.

This article intends to offer a review of the research development in relation to capacitive electrode materials and EES device design innovation, leading to the energy capacity improvement of capacitive EES devices including supercapacitor and supercapattery. The authors' research group has studied supercapacitors and supercapatteries for more than a decade at the electrode material level and the device level in series. The examples in this review article are mainly chosen from the authors' publications on supercapacitors and supercapatteries, accompanied with the recent progress on the high energy capacity electrode materials.

One type of supercapacitors called 'electrical double layer capacitor (EDCL)' can directly store electrical energy at two activated carbon (Act-C) electrodes and output a high specific power like 90 $kW \cdot kg^{-1}$, but a specific energy range of 2 ~ 8 $Wh \cdot kg^{-1}$, which can be improved by using the pseudocapacitor[2]. In some conditions, the electrode materials used in batteries can also be used in supercapacitors and supercapatteries, while in the battery community 'anode' and 'cathode' are quite often utilised in place of negative and positive electrodes, respectively[12]. The use of the anode and cathode notions is correct when the discharging behaviour is emphasised in battery studies, but may cause confusion in capacitive device studies where anode or cathode cannot precisely describe the electrical polarities of electrodes, for example it is impossible to know whether the potential of an anode is higher or lower than that of a cathode. To avoid this confusion, positrode and negatrode have been proposed in place of positive electrode and negative electrode, respectively.

1 Positrode Materials

In EDLC studies, Act-Cs have been widely used as both positrode and negatrode materials to reveal the fast charging and discharging performance. Pseudocapacitive materials such as electronically conducting polymers (ECPs) and transition metal oxides (TMOs) based on their nanostructured, redox active, and semiconductive natures, have been applied in supercapacitor and supercapattery studies to improve the energy capacities of these capacitive EES devices. In this section, we focus on the ECPs and TMOs as the positrode materials in the capacitive EES device studies. As to the Act-C positrode, we will discuss the details in the sections of Negatrode and Electrode Mass Balance and Supercapattery.

1.1 ECPs Positrode Materials

ECPs can boost the capacitance because they are redox active, and can utilise fast and reversible electron transfer or Faradic reactions for charge storage within the electrode. It is clear that the ECPs can serve as both positrode and negatrode materials in supercapacitor studies, but their capacitive potential ranges are normally narrower and more positive than the ones of Act-Cs, indicating ECPs can take more advantages to serve as the positrode materials than Act-Cs in supercapacitor. However, ECPs perform quite below expectation when they are used alone without any morphology control and hybridisation with other materials, similar to carbon nan otubes (CNTs) and graphene. The ECP, poly(3,4-ethylenedioxythiphene) (PEDOT), is a typical example that the pure PEDOT was reported in 1990s to be able to exhibit rectangular shape cyclic voltammograms (CVs) like a capacitor, but the symmetrical PEDOT supercapacitor offered fairly specific energy of 1 ~ 4 $Wh \cdot kg^{-1}$ at that time, while the goal was set to be 15 $Wh \cdot kg^{-1}$[14]. A comparison in the theoretical and experimental specific capacitances of polyaniline (PAn) was done in a previous study, suggesting that the porosity and heterogeneous structure of PAn can be the main factors for the much lower values of experimental specific capacitance than the theoretical one[15]. There are several strategies to improve the capacitance performance of the ECPs in the subsequent studies on supercapacitor electrode materials, including manipulation of the morphology of ECPs[16-18], and hybridisation of the ECPs and the other materials[19-21].

Following the morphology strategy, the polypyrrole (PPy) nanowires and nanofibers were synthesised by electrochemical deposition[16] and near-field electrospin[17], respectively. The achieved all-polymer micro supercapacitor demonstrated a better performance than the other materials[16]. A 3D hierarchical PAn micro/nanostructure as supercapacitor electrode material was also reported based on the morphology strate gy to improve the ECPs's performance[18]. In this study, the additional salt and low temperature, as well as the depressed diffusion kinetics caused by the frozen reaction system were considered to contribute the formation of the hierarchical structure of PAn[18], whose specific capacitance reached 520 $F \cdot g^{-1}$ at 0.5 $A \cdot g^{-1}$.

Combining CNTs with ECPs were found to be able to overcome the drawbacks of ECPs in mechanical strength and conductivity, and maintain their large pseudocapacitance[21]. The hybrids can be synthesised by electrochemical co-deposition[21-29] and chemical methods[30-32], respectively. The skeleton materials in the hybrids are not limited to CNTs, but also graphene[33-34] and other carbon based materials[35-36].

During the electrochemical co-deposition process, the ionised CNTs via partial oxidation in an acid were used as the dopant when ECPs were electrochemically deposited on the surface of the electrode forming CNT-ECP hybrids. For example, a stabilised aqueous solution containing ionised CNTs and pyrrole monomers was used in the electrochemical co-deposition of the composites of CNTs and PPy[21]. The ionised CNTs act as the supporting electrolyte in the solution and also the electron conductive dopants in the CNT-PPy hybrids. Fig.1A and 1B show the high-resolution transmission electron microscopic (HRTEM) and scanning electron microscopic (SEM) images of the CNT-PPy hybrids, respectively. The TEM sample was prepared by electrolysis at a low potential for a short time using a bare copper grid suspended on a platinum wire as the working electrode, while the SEM sample was prepared on a graphite disc electrode. The TEM image clear indicates two almost parallel nanotubes coated by a layer of PPy. The SEM image shows various conditions including (1) a relatively rare section of a CNT that had not been coated by the end of the experiment, (2) a fully coated CNT, (3) a coated nanoparticles, and (4) a join between a coated CNT and another coated nanoparticle or CNT.

A schematic illustration is shown in Fig. 2 to summarise the procedures used in our research group for electrochemical co-deposition of the composite films with acid treated (ionised) CNT and ECPs, including PPy, polyaniline (PAn) and PEDOT. A systematic and comparative study of the electrochemical synthesis and capacitance of CNT composites with PPy, PAn, and PEDOT has been taken to understand the similarities and differences between these CNT composites with different polymers[28-30, 37]. In general, the comparison of the CNT-ECPs can be made by various experimental methods such as CV, electro chemical impedance spectroscopy (EIS), and electrochemical quartz crystal microbalance (EQCM). Table 1 demonstrates a detailed comparison of the electrochemically co-deposited CNT-ECPs and pure ECPs.

As shown in Fig. 2, solutions with acetonitrile or a mixture of acetonitrile and water as the solvent were used in the electrochemical co-deposition with CNTs because of the insolubility of EDOT monomer

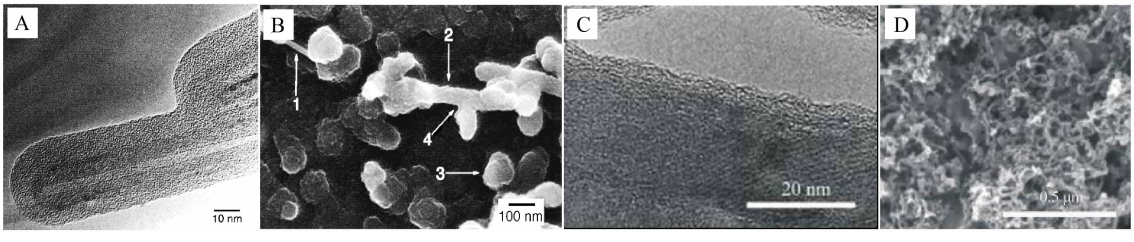

Fig. 1 HRTEM (left) and SEM (right) images of electrodeposited (A, B)[21] and chemically synthesised (C, D)[32] CNT-PPy hybrids

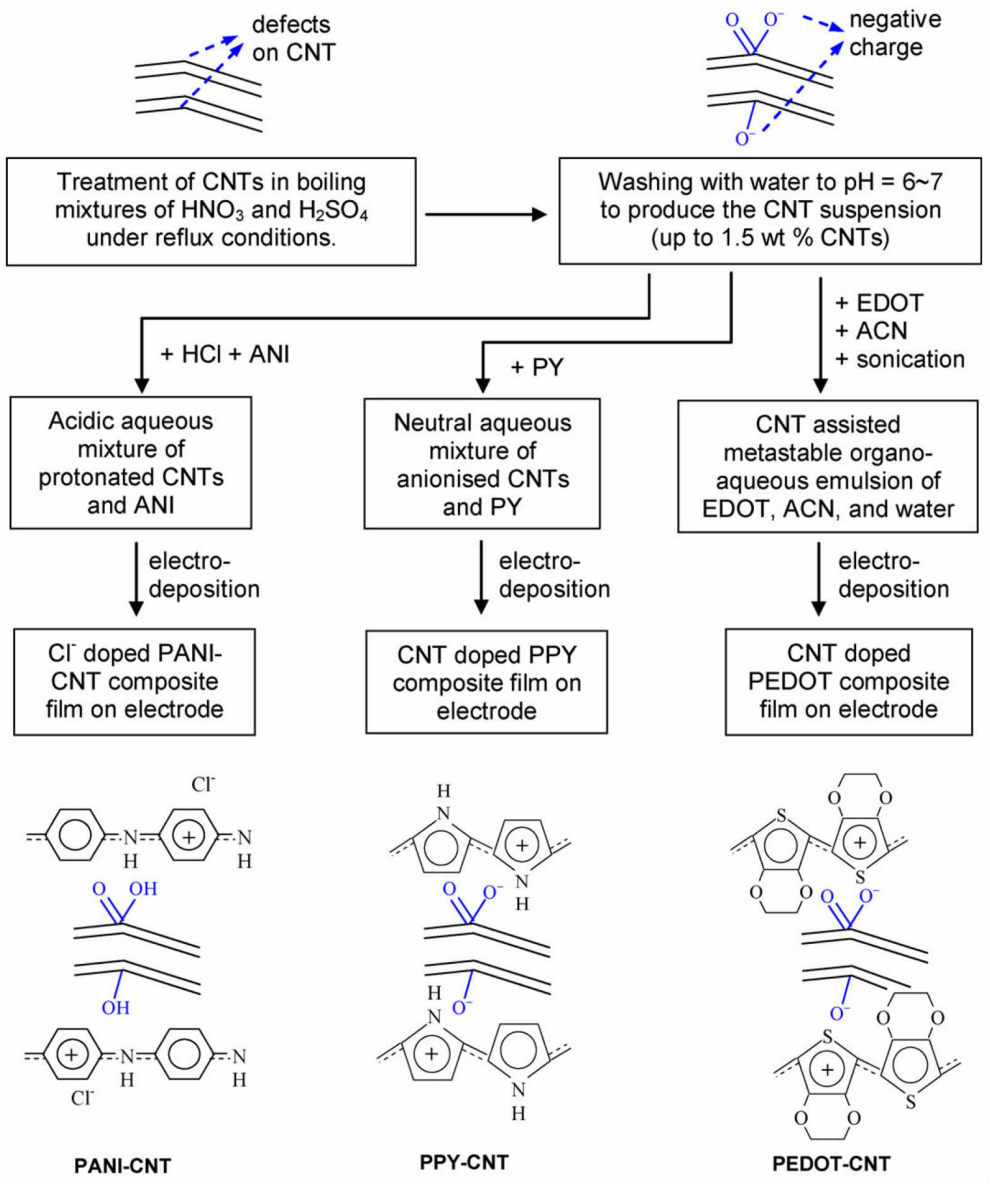

Fig. 2　Schematic illustration of the procedures used for electrochemical co-deposition of the composite films with ECPs and acid treated (ionised) CNT. ACN: acetonitrile.[29]

in water[26, 28-29]. Although additional supporting electrolyte was added in the solution, the CNTs in the mixture of the acetonitrile and water helped formation of sufficiently stable emulsion by sonication. The emulsion would eventually separate into different phases only after a long time as shown in Fig. 3[29]. The sufficiently stable emulsion enabled the aforementioned co-deposition of CNT-PEDOT composites and relevant investigation on their capacitance and morphology[26-29].

A thick, coherent, and porous PEDOT coating up to 0.5 mm on a platinum electrode could be electrochemically deposited, and the deposited PEDOT film exhibited a linearly increasing electrode capacitance, approaching 5 $F \cdot cm^{-2}$, against the deposition charge, and the capacitance values measured by CV and EIS are comparable in every deposition charge condition as shown in Fig. 4. It should be mentioned that this electrode capacitance of PEDOT is much higher than the reported electrode capacitances of PPy and PAn, even though the latter two are much larger in specific capacitance ($F \cdot g^{-1}$). On this base, the

Tab. 1 Electrochemical data for thin films of conducting polymers and their composites with acid treated CNTs*[29]

Parameter	CNT-PAn	PAn	CNT-PPy	PPy	CNT-PEDOT	PEDOT
Deposition charge, Q_{dep}/mC	6.5	6.5	6.5	6.5	6.5	6.5
Capacitive potential range, U/V	0.65	0.65	1.00	1.00	1.00	1.00
CV capacitance, C_{CV}/mF	1.31	1.20	1.44	0.51	1.17	0.54
EIS capacitance, C_{EIS}/mF	1.27	1.05	1.10	0.47	0.79	0.39
EIS bias/V(vs. Ag/AgCl)	0.60	0.60	0.40	0.40	0	0
C_{EIS}/Q_{dep}/(F/C)	0.195	0.162	0.169	0.072	0.122	0.060
Knee frequency/Hz	66.0	66.0	829.0	49.4	268.0	28.1
Z' at 0.01 Hz/Ω	52.5	58.4	212	397	200	581

*Each film was electrochemically deposited on a Pt disc electrode with a surface area of 0.02 cm^2.

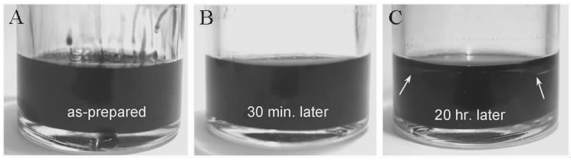

Fig. 3 Photographs showing the metastable emulsion of mixed 0.25 mol·L^{-1} EDOT in acetonitrile and 0.3w.% CNT aqueous suspension (1:1, v:v), which were taken (A) immediately after sonication, (B) 30 min and (C) 20 h after keeping the mixture stationary in air. Noted that visible phase separation can be only found in (C) as indicated by the arrows.[29]

CNT-PEDOT composite also exhibited a linearly increasing electrode capacitance which was significantly bigger than the pure PEDOT[26]. This finding helped us to understand the practical performance of the electrode materials in supercapacitor. In practice, we can notice that the capacitance of a supercapacitor does not simply increase linearly with increasing the amount of the active electrode material. It is impossible to gain higher capacitance by increasing the mass after the thickness has reached the kinetic limit, which is related to the ion intercalation and depletion in the charge-discharge processes. In this case, evaluation of the electrode performance cannot always be appropriate by only using specific capacitance. The electrode capacitance can be a complementary evaluation parameter, which measures the practically accessible capacitance over an unit geometric area of the electrode substrate.

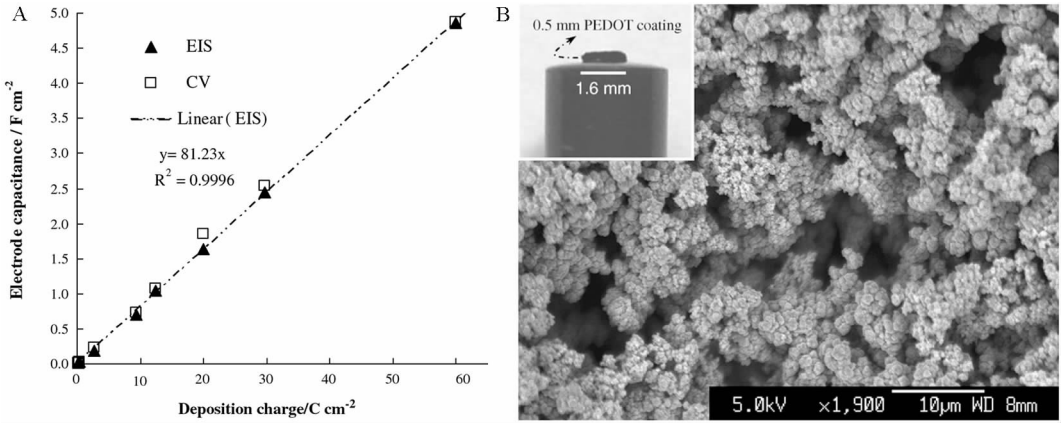

Fig. 4 A. Electrode specific capacitance as a function of PEDOT film deposition charge[27]. Values measured by both EIS (filled triangles) and CV (unfilled squares) are presented. B. SEM image of the top view of a potentiostatically grown PEDOT film (deposition charge: 30 C·cm^{-1}) and photograph of the side view of a PEDOT film (60 C·cm^{-1}) on a Pt disc electrode[27].

EQCM can investigate the accurate mass change on the electrode during the electrochemical reaction processes. A detailed investigation on processes of electrodepositing CNT-PPy and pure PPy film in potassium chloride (KCl) solution and pure PPy in tetrabutylammonium bromide (NBt_4Br) solution was done to understand the role of ionised CNTs in the polymerisation[24]. The CVs and mass-potential plots of the PPy and CNT-PPy films are compared in Fig. 5. It can be noticed that the only anion uptake and expulsion were observed for the PPy film in NBt_4Br solution as shown in Fig. 5A and 5B, whilst clear cation expulsion and anion uptake were seen for CNT-PPy film in KCl solution as shown in Fig. 5C and 5D. This evidence clarified the doped CNTs in the CNT-PPy composites.

EQCM can also measure the specific capacitance of the CNT-ECP composites. It was found that the specific capacitance of CNT-PPy film, 200 $F \cdot g^{-1}$, was slightly lower than that of the similarly grown PPy film, 240 $F \cdot g^{-1}$[24]. These results are reasonable once the inclusion of redox inert CNTs in the composite film is considered. The specific capacitances of the electrodeposited PAn and PEDOT thin films were also determined by EQCM to be 530 and 92 $F \cdot g^{-1}$, respectively. More quantitative analysis is pending for the knowledge of the CNT content in the CNT-ECP composites.

Although the electrochemically co-deposited CNT-ECP composites have exhibited satisfied performances and are good for lab work, there are still a lot of challenges to reveal mass-production by the electrochemical methods. Chemical synthesis of the CNT-ECP composites can be convenient and readiness. The main challenge is the presence of homogeneously dispersed CNTs in the reaction solution before and during the chemical polymerisation[31-32]. The HRTEM and SEM images of chemically synthesised CNT-PPy composites, as shown in Fig. 1C and 1D, demonstrated a successful case. A homogeneous PPy layer was covered on the CNTs surface in the chemically synthesised CNT-PPy composites, similar to the case of electrochemically co-deposited CNT-ECP composites. It provides strong evidence that the ECPs were attached to the CNTs through not only the negatively charged surface groups of CNTs, but also the π-π stacking because chemical bonds in both ECPs and CNTs are highly conjugated.

Another characteristic of the chemically synthesised CNT-ECP composites is the powdery product that requires further steps for fabrication of the elec trode. Screen printing can be a feasible process for fabricating the electrode. However, a challenge for looking for a suitable binder and possibly a surfactant that can help disperse the CNT-ECP powders into a stable ink came with the screen printing of the CNT-ECP electrode. The binder and surfactant normally have no contributions to the capacitance and conductivity of the electrode due to their non-reactive and non-conductive natures. It was found that the binder had to be more than 15 % of the active materials, and this situation will lower the energy capacity of the electrode which is the main concern in supercapacitor studies. Identifying and developing a suitable route for fabrication of the chemically synthesised CNT-ECP composite powders into the electrode should be one of the main tasks in future studies.

Except for CNTs, the other carbon materials, like graphene, Act-Cs, and carbon quantum dots, were used to synthesise ECP composites. In a recent report, PAn was synthesised exclusively inside the micropores of Act-Cs[20]. The nanostructured PAn was smaller than 2 nm in diameter and allowed for fast redox reactions. Although the PAn underwent swelling and shrinkage during the charging and discharging processes, the carbon pore walls were able to absorb the expansion of PAn during the charging process, and this Act-C-PAn composite exhibited superior capacitance in terms of specific power and energy, and excellent cycle lifetimes. It was found that carbon quantum dots can also improve the capacitance performance of the PAn composites, whose specific capacitance reached 738 $F \cdot g^{-1}$ at 1.0 $A \cdot g^{-1}$[19]. The high capacitive performance of this PAn composite was ascribed to the incorporation of carbon quantum dots,

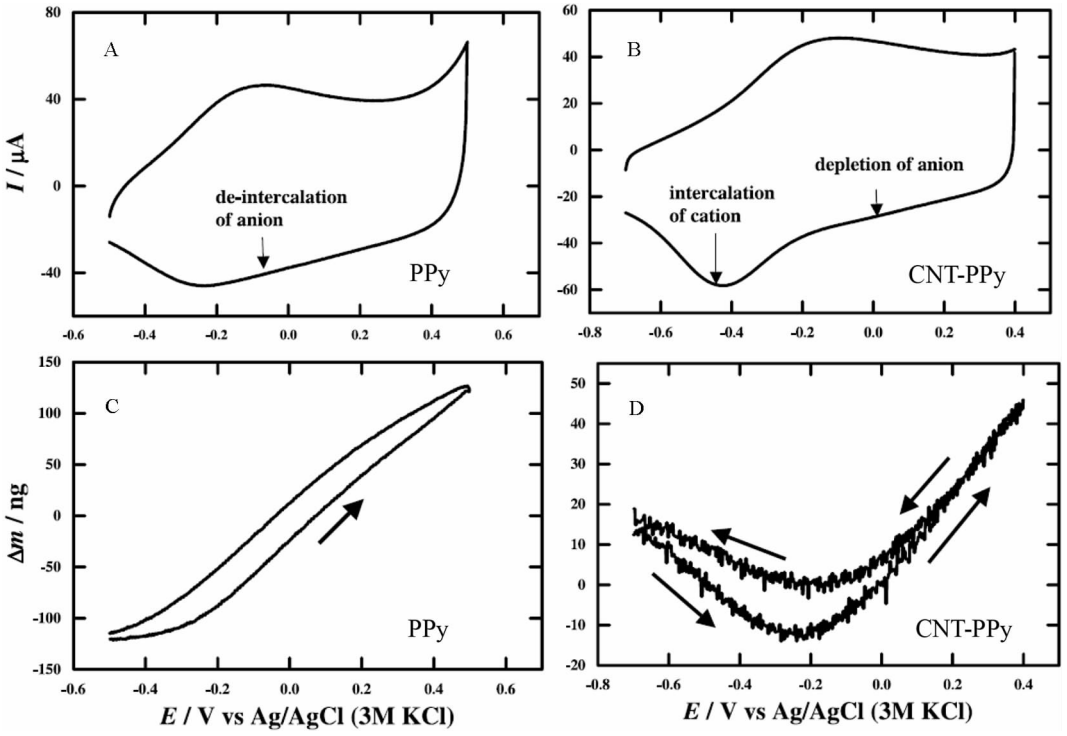

Fig. 5 CVs (A, B) and the simultaneously recorded mass-potential plots (C, D) of pure PPy in 0.5 mol·L^{-1} tetrabutylammonium bromide (A, C) and the CNT-PPy composite in 0.5 mol·L^{-1} KCl. Potential scan rate: 50 mV·s^{-1}. Both the PPy and CNT-PPy coatings were electro-deposited.[24]

which improve the conductivity of PAn composite, and alleviate the swelling and shrinkage during the charging and discharging processes.

1.2 TMOs Positrode Materials

Ruthenium dioxide (RuO_2) was possibly the first published redox active materials to be able to exhibit rectangular CVs like a capacitor in 1971[38]. The follow-up works clarified that amorphous RuO_2 can exhibit excellent pseudocapacitance behaviour with high specific capacitance and great reversibility[39-40]. The commercial application of this precious TMO will be very uneconomic due to the low abundance of Ru in earth and the corresponding high cost of this TMO. It is obviously needed to look for cost-effective pseudo-capacitance TMO electrode materials. Manganese dioxide (MnO_2) basically satisfies the aforementioned criteria, and has been widely used as the positrode materials in battery, supercapacitor, and supercapattery studies. Previous work claimed that thin MnO_2 film can possess a specific capacitance of 698 F·g^{-1}[41]. The capacitive MnO_2 electrode materials can be prepared through several synthesis routes, one of which is based on the redox deposition of MnO_2 on carbon based materials[42-45]. The carbon based materials can be graphite, CNTs, graphene, and Act-Cs. It was concluded that Reaction (1) was the dominate reaction for the redox deposition of MnO_2 when the carbon based materials react with a potassium permanganate ($KMnO_4$) neutral aqueous solution.

$$4MnO_4^- + 3C + H_2O \rightarrow 4MnO_2 + CO_3 + 2HCO_3 \quad (1)$$

In an early study, the thin MnO_2 films were prepared by immersing a graphite disc electrode in a stirred solution of 0.25 mol·L^{-1} $KMnO_4$ containing 0.5 mol·L^{-1} sulfuric acid (H_2SO_4)[42]. Both the thickness and electrode capacitance of the prepared electrodes linearly increased against the reaction time. The electrode capacitance of such MnO_2 coated electrode reached 45 mF·cm^{-2} with the deposition time up to 60 min that obey well the logarithm law in 0.5 mol·L^{-1} lithium chloride (LiCl) solution. Further investigation of the electrode capacitance in various neutral aqueous electrolytes revealed that there is a clear reverse

trend of the increasing electrode capacitance against the decreasing size of the alkali metal cations. This preliminary work firstly reported the specific capacitance of the MnO_2 thin films on the graphite disc electrode by using redox deposition method at that time, and accurately predicted the follow-up work in redox deposition of MnO_2 on CNTs[43] and graphene[46]. More details can be found from Table 2, which lists the specific capacitances calculated from the CVs collected from the MnO_2 coated electrode in various aqueous electrolytes.

A nanoscale micro-electrochemical cell mechanism was proposed to describe the reaction processes of producing CNT-MnO_2 composites by adding a $KMnO_4$ solution into a CNT suspension. The postulated mechanism is schematically illustrated in Fig. 6A and 6B, indicating the initial and later stages of direct contact reaction between MnO_4^- and CNT defect and/or tube end. At the initial stage shown in Fig. 6A, the reduction of MnO_4^- is not favourable because of a local increase of pH and depletion of MnO_4^- at the reaction sites.

The electron transfer through CNTs in the later stage shown in Fig. 6B constitutes the micro-electrochemical cell postulation that the CNTs make the defect and another location on the CNT wall to be the anode and cathode, respectively. The HRTEM and TEM observations from Fig 6C and 6D can prove the postulation, showing clearly the CNTs possessing an open end without any MnO_2 coating and CNTs with

Tab. 2 The capacitances of a redox-deposited MnO_x film on graphite in different electrolytes[42]

	LiCl	$LiClO_4$	NaCl	NaCl	NaCl	Na_2SO_4	Na_2SO_4	KCl	KCl
Electrolyte/(mol·L^{-1})	0.5	0.5	0.5	1.0	2.0	0.1	0.25	0.5	1.0
Capacitance*/(mF·cm^{-2})	8.9	8.3	7.1	5.7	5.6	7.6	7.6	6.8	5.8

*All capacitance data were derived from the stable cyclic voltammograms of the same electrode that was obtained after 2 min redox deposition. The electrode was thoroughly washed by water between experiments.

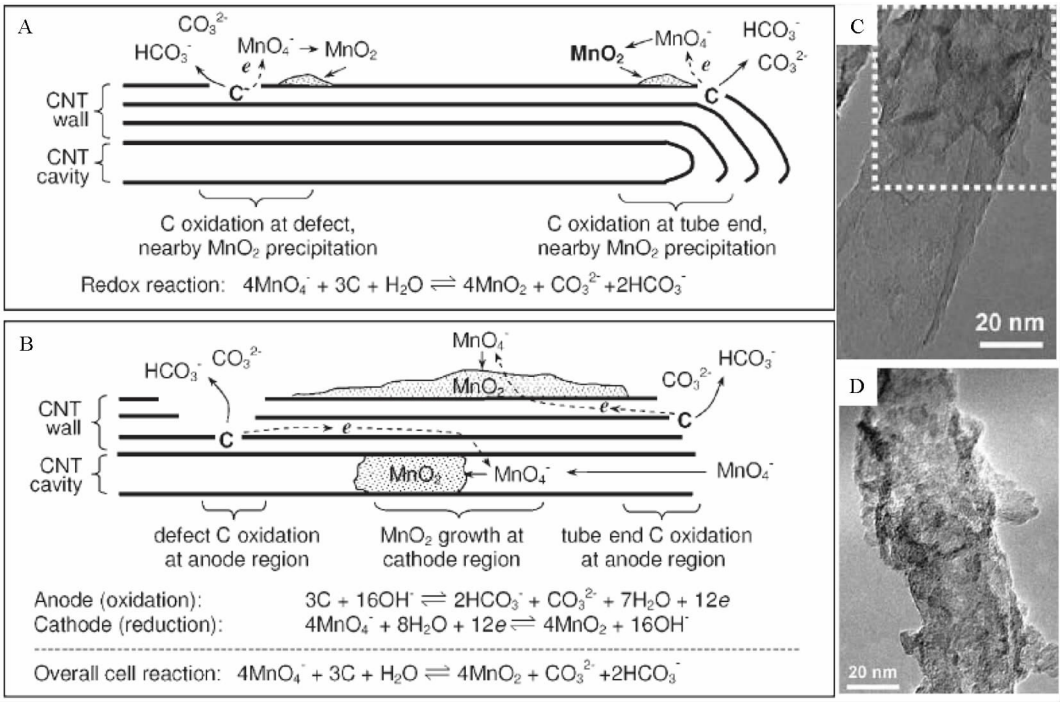

Fig. 6 Schematic illustration of redox deposition. (A) initial stage, (B) later stage and typical TEM images of (C) a corroded CNT ends with selective coated nanocrystalline MnO_2 and (D) a CNT with MnO_2 coating (50w.% MnO_2).[43]

50wt.% MnO_2 coating.

A series of CVs for the CNT-MnO_2 composites electrode are shown in Fig. 7. The composite was loaded on a trenched graphite disc electrode, and the composite electrode maintained 93% of the original capacitance after 200 cycles and 91% after 9000 cycles. The initial fast capacitance loss may be associated with morphological changes in the composite resulting from repeated charging-discharging accompanied by the absorption-desorption of the counter ions. In general, the CNT-MnO_2 composites showed a good performance as a positrode, whose specific capacitance of the CNT-MnO_2 composites was 144 $F \cdot g^{-1}$ on average, and the electrode capacitance of 5 $F \cdot cm^{-2}$ was a very high value when the paper was published[43]. A symmetrical supercapacitor stack was designed using bipolar plate as the current collector. Table 3 summarises the general performance of the symmetrical single cell and two-cell stack. The Equivalent Series Resistance (ESR) of the cell stack is smaller than the double of the value of the single cell, indicating the benefit from bipolarly stacking the individual cells.

2 Negatrode Materials and Electrode Capacitance Balance

If a symmetrical cell made of the aforementioned composites was built, the positrode and negatrode have to share the same working potential range[30], leading to a smaller working voltage, which is directly related to the cell energy capacity based on the energy equation for capacitor, $E = CU^2/2$, where C is the specific capacitance and U the maximum charging voltage of the capacitor. Numerous attempts have been made to increasing the energy capacity of the supercapacitors, including developing new materials with high C and extending U of relevant super-

Tab. 3 Performance comparison of symmetrical single cell and two-cell stack[45]

Symmetrical CNT-60 w.% MnO_2	Single cell	Two-cell stack
Capacitance (CV, 10 $mV \cdot s^{-1}$)	0.49 F	0.21 F
Capacitance (EIS, 0.0 V)	0.53 F	0.23 F
Capacitance (GCD, 10 $mA \cdot cm^{-2}$)	0.50 F	0.20 F
Applied cell voltage	0.9 V	1.8 V
Equivalent Series Resistance (from EIS at 0 V)	0.62 Ω	1.08 Ω
Charge- transfer resistance	0.55 $\Omega \cdot cm^{-2}$	1.06 $\Omega \cdot cm^{-2}$
Coulombic efficiency (10 $mA \cdot cm^{-2}$)	96.6 %	95.6 %

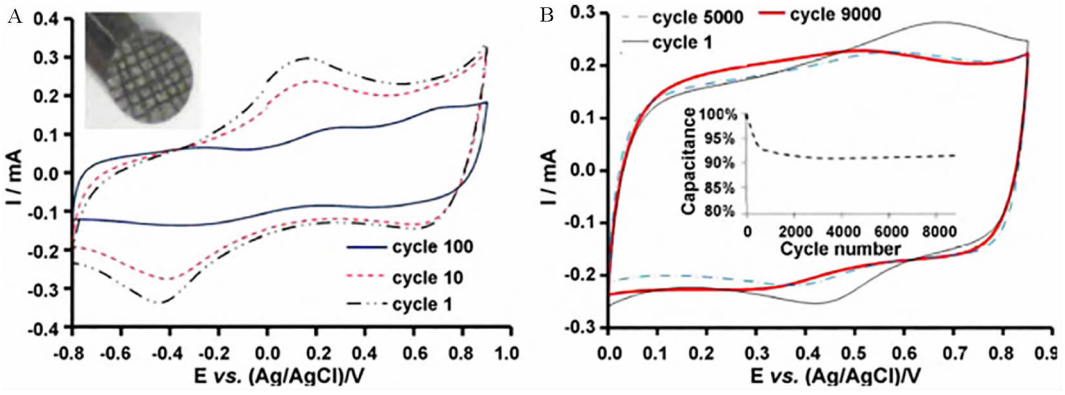

Fig. 7 CVs of CNT-MnO_2 composite with 65w.% of MnO_2 in 0.5 $mol \cdot L^{-1}$ KCl recorded during continuous potential cycling in the potential ranges of (A) -0.80 to 0.90 V (the inset: photo of the trenched graphite disk electrode) and (B) 0.0 ~ 0.85 V (the inset: a plot of the relative capacitance against the number of potential cycle.[45]

capacitors. It was found that device design can greatly affect the energy capacity of the designed supercapacitor by using unequalised electrode capacitances in asymmetrical super capacitors. In general, the CNT-ECP or CNT-TMO composites discussed in the previous sections can act well as the positrode materials, and the negatrode will be made of the materials whose capacitive potential range (CPR) is more negative than the one of the aforementioned positrode composites. A model of supercapacitor voltage is schematically illustrated in Fig. 8[37], where the lower and upper potential limits of the negatrode and positrode are denoted as E_{N1}, E_{N2}, E_{P1}, E_{P2}, respectively. Act-Cs, specially structured carbons, and TMOs [47] processing relevant negative CPR have been selected as the negatrode materials in supercapacitor studies. For example, a hybrid energy storage device combining graphene-Fe_3O_4 composite negatrode with 3D graphene based positrode exhibited specific energy of 204 ~ 65 Wh·kg^{-1} over the specific power from 55 to 4600 W·kg^{-1}[47]. In this hybrid, the graphene-Fe_3O_4 is a battery electrode material, whilst the 3D graphene is a capacitive material. The details in this kind of device will be discussed latter in the section of Supercapattery.

A carbon black, Cabot Monarch 1300 pigment black (CMPB), is a form of paracrystalline carbon whose specific capacitance was found to be 114 F·g^{-1}, and the CMPB electrode can exhibit a high overpotential for the reduction of the H^+ ion, pushing the potential to be more negative than -0.65 V vs. Ag/AgCl[30]. Based on the understanding illustrated in Fig. 8, CNT-PAn and CMPB were used as positrode and negatrode materials, respectively, for asymmetrical supercapacitors, where the CNT-PAn positrode was found to be the 'cell voltage limiting electrode'[30]. It was found that the maximum charging voltage (MCV) of an asymmetrical supercapacitor made of CNT-PAn positrode and CMPB negatrode can be extended by increasing the capacitance of the positrode (CP) with the fixed capacitance of the negatrode (CN) as shown in Fig. 9, where the MCV increased from 0.97 to 1.65 V with the ratio of CP/CN increasing from 0.8 to 1.5. Similar effect can also be found in the supercapacitors made of CNT-PPy positrode and CMPB negatrode[32].

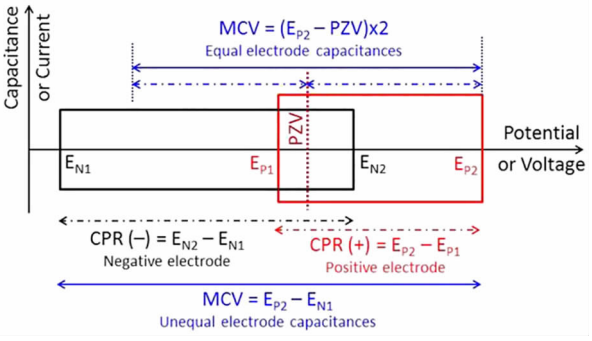

Fig. 8 Schematic illustration of supercapacitor maximum charging voltage (MCV), potential zero voltage (PZV), and electrode capacitance potential range (CPR: E_{N2}-E_{N1} or E_{P2}-E_{P1} for the negatrode and positrode, respectively).[37]

In a reported asymmetrical carbon-carbon supercapacitor, MCV reached 1.9 V in a test up to 10000 charging-discharging cycles with a stabilised capacitance value after 1000 cycles[48], while a symmetrical carbon-carbon supercapacitor can only be charged to 1.6 V using the same aqueous electrolyte but in different concentrations[49-50]. A good wettability of aqueous electrolyte on Act-C electrodes can have a positive effect on the energy storage performance of su percapacitors[51]. However, some of the binders are hydrophobic and have to be used for Act-Cs in the electrode fabricating processes, leading to a poor energy storage performance of the relevant electrodes or devices. Addition of iso-propanol in an aqueous electrolyte containing 1.0 mol·L^{-1} Na_2SO_4 was found to be able to minimise the electrolyte surface tension, and hence maximise the wettability of the electrolyte on the Act-C powders. The drops of aqueous electrolyte with or without additional iso-propanol demonstrated different wetting angles on the die-pressed Act-C pellets (containing 5wt.% polytetrafluoroethylene, PTFE) of different densities as shown in Fig. 10[51]. First, the amphiphilic iso-propanol can facilitate the impregnation of the pores inside the Act-C pellet by the aqueous electrolyte. Second, increasing the porosity with decreasing the density of the Act-C pellet

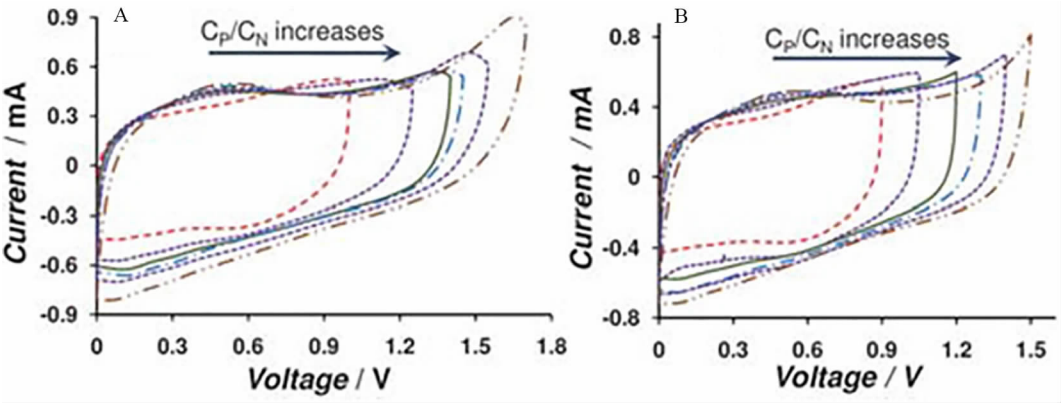

Fig. 9 CVs of asymmetrical supercapacitors with a 0.3 mg CMPB negatrode and a CNT-Pan positrode at various CP/CN ratios (0.8, 1.0, 1.1, 1.2, 1.3, 1.5) with (A) and without (B) the charging current peak. Scan rate: 20 mV·s^{-1}.[30]

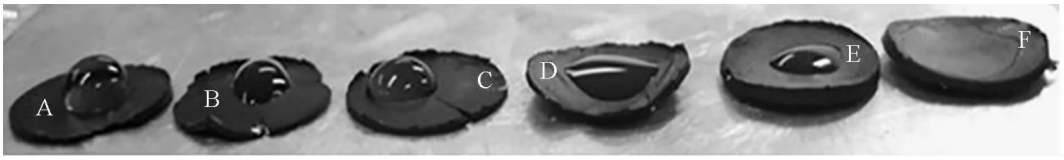

Fig. 10 Photograph showing drops of the 1.0 mol·L^{-1} Na_2SO_4 solution without (A, C, E) and 8 vol.% added iso-propanol (B, D, F) on Act-C pellets of different apparent densities and the same weight (0.05 g): 0.35 g·cm^{-3} (E, F), 0.55 g·cm^{-3} (C, D), 0.70 g·cm^{-3} (A, B).[51]

will help the same impregnation process.

3 Supercapattery

In the recent decade, supercapattery has been proposed as a new term to represent a wide range of capacitive EES devices including any kinds of pseudocapacitors and capacitive hybrids of a highly polarisable capacitor-like electrode (i.e., it has a wide potential window) and a battery-like electrode. Supercapatteries take advantages of both capacitive and Faradaic charge storage mechanisms at either the electrode material level or, more often, the device level. At the materials level, the aforementioned ECPs or TMOs composite can be used for supercapattery, suggesting that pseudocapacitors consisting of two electrodes of the same (symmetrical) or different (asymmetrical) pseudocapacitive materials can be just considered as a special case of supercapatteries. In such hybrids, the capacitor-like electrode offers the EDLC or pseudocapacitance or both, and the battery-like electrode contributes either pseudocapacitance or non-capacitive charge storage via redox or Faradaic reactions. All these attempts aimed to achieve the high power capability of supercapacitors and the large storage capacity of batteries[13]. In some recent literatures, the other definition like hybrid electrochemical capacitor[52] and supercapacitor-battery hybrid[47] were used to describe supercapattery. In these reports, either pseudocapacitive or non-capacitive electrode material was used in the hybrid device, demonstrating the outstanding energy capacity. The authors reported the preliminary tests of a supercapattery with an Act-C positrode, a lithium metal negatrode and an ionic liquid electrolyte of $LiClO_4$, revealing a MCV of 4.2 V and minimum discharging voltage of 1.7 V. The galvanostatic charging-discharging (GCD) curves of this supercapattery are shown in Fig. 11, and the specific energy derived from this figure is beyond 230 Wh·kg^{-1} under the GCD current density of 1.0 mA·cm^{-2}[10].

4 High MCV Capacitive EES Devices

A lot of power devices require high voltage, but the MCV values of the capacitive EES devices are determined by the electrode materials and elec-

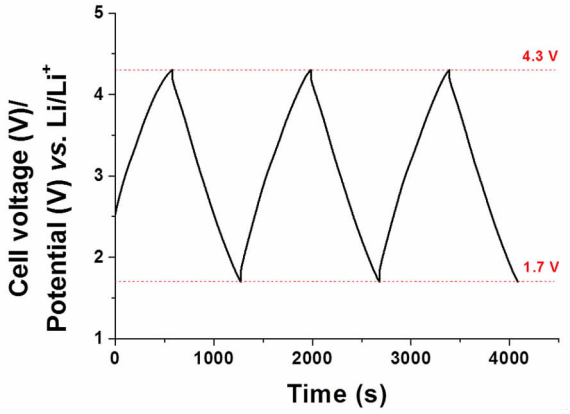

Fig. 11 Galvanostatic charging-discharging curves for an experimental demonstration of supercapattery, Li metal (-)|Ionic Liquid (Li^+)|Act-C (+), under a current density of 1.0 mA·cm^{-2}[10].

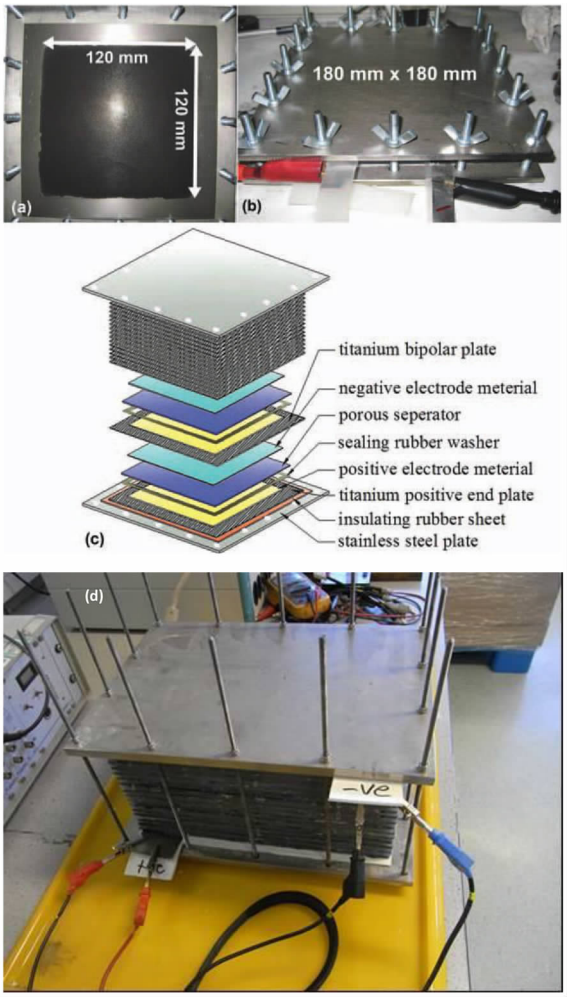

Fig. 12 Photographs of (A) a middle titanium bipolar plate in the stack loaded with CNT-PPy composite, and (B) the stack of 19 CMPB (-)|3 mol·L^{-1} KCl|CNT-PPy (+) supercapacitors connected through titanium bipolar plates[31]. (C) The expanded schematic illustration of the bipolarly connected stack[31]. (D) Photograph of a 22 V stack consisting of 16 supercapacitors using graphite bipolar plates in authors' laboratory.

trolytes. A high MCV beyond 4.0 V of the supercapattery with organic electrolytes can be achieved, whilst the MCV of supercapacitors fall within the scope of 1.0 ~ 2.0 V with aqueous electrolyte s and 2.0 ~ 4.0 V with organic electrolytes. An approved strategy is to serially stack the cells through bipolar electrodes. A prototype stack composed of 19 home-made supercapacitors connected through titanium bipolar plates was fabricated and demonstrated in the authors' lab. Fig. 12A and 12B show the photographs of the homemade active materials with titanium bipolar plate and the stack of 19 supercapacitors connected through titanium bipolar plates. An expanded schematic illustration is shown in Fig. 12C. This 19-cell stack achieved 20 V without noticeable unwanted electrode reactions. The ESR of the stack could be as low as 0.30 Ω. The maximum specific power and specific energy of the stack reached 24.71 kW·kg^{-1} and 3.64 Wh·kg^{-1}, respectively. The stack showed very high charging-discharging cycle stability, with the capacitance loss being almost zero in the 10 V range and less than 6% in the 10 V range after 1000 cycles. The device has been stored in the author's lab for more than 5 years, and it still works. The titanium plate can be replaced by graphite plates and the CMPB negatrode replaced by Act-C negatrode to achieve higher MCV, leading to a 22 V demonstration of supercapacitor stack with 16 cells as shown in Fig. 12D.

5 Conclusions

This article has introduced several recent attempts to improve the energy capacity of the capacitive EES devices, including supercapacitor and supercapattery, at both the electrode materials level and device level. In the past two decades, different kinds of ECPs and TMOs composites have been studied and used as the positrode materials to increase the specif-

ic capacitance of the electrode, and hence the energy capacity of the relevant supercapacitors. Supercapatteries have been proposed, and preliminarily demonstrated and tested. The hybrid structure of supercapattery is an innovation on the EES devices. The redox materials in supercapattery play an important part of providing the high energy capacity. Bipolar plate stack technology for supercapacitor is also reviewed here. These bipolarly connected supercapacitor stack can effectively increase the MCV to meet the high voltage demand from the power devise.

Acknowledgements

This work has received funding supports from Ningbo Municipal Government (3315 Plan and IAMET Special Fund, 2014A35001-1, and Ningbo Natural Science Foundation Programme, 2016A610115) and Zhejiang Provincial Applied Research Programme for Commonweal Technology, 2016C31023 and 2017C31104.

References:

[1] Kammen D M, Sunter D A. City-integrated renewable energy for urban sustainability[J]. Science, 2016, 352(6288): 922-928.

[2] Stevenson A J, Gromadskyi D G, Hu D, et al. Supercapatteries with hybrids of redox active polymers and nanostructured carbons[M]// Nanocarbons for Advanced Energy Storage. Wiley-VCH Verlag GmbH & Co. KGaA; 2015: 179-210.

[3] Grey C P, Tarascon J M. Sustainability and *in situ* monitoring in battery development[J]. Nature Materials, 2017, 16 (1): 45-56.

[4] Liu W, Song M S, Kong B, et al. Flexible and stretchable energy storage: Recent advances and future perspectives[J]. Advanced Materials, 2017, 29(1): 1603436.

[5] Larcher D, Tarascon J M. Towards greener and more sustainable batteries for electrical energy storage[J]. Nature Chemistry, 2015, 7(1): 19-29.

[6] Wang Y, Zhong W H. Development of electrolytes towards achieving safe and high-performance energy-storage devices: A review[J]. ChemElectroChem, 2015, 2(1): 22-36.

[7] Zhang K, Han X, Hu Z, et al. Nanostructured Mn-based oxides for electrochemical energy storage and conversion[J]. Chemical Society Reviews, 2015, 44(3): 699-728.

[8] Salanne M, Rotenberg B, Naoi K, et al. Efficient storage mechanisms for building better supercapacitors[J]. Nature Energy, 2016, 1: 16070.

[9] Wen L, Li F, Cheng H M. Carbon nanotubes and graphene for flexible electrochemical energy storage: From materials to devices[J]. Advanced Materials, 2016, 28(22): 4306-4337.

[10] Yu L P, Chen G Z. High energy supercapattery with an ionic liquid solution of $LiClO_4$[J]. Faraday Discussions, 2016, 190: 231-240.

[11] Yu L P, Chen G Z. Redox electrode materials for supercapatteries[J]. Journal of Power Sources, 2016, 326: 604-612.

[12] Chen G Z. Supercapacitor and supercapattery as emerging electrochemical energy stores[J]. International Materials Reviews, 2017, 62(4): 173-202.

[13] Guan L, Yu L, Chen G Z. Capacitive and non-capacitive faradaic charge storage[J]. Electrochimica Acta, 2016, 206: 464-478.

[14] Carlberg J C, Inganas O. Poly(3,4-ethylenedioxythiophene) as electrode material in electrochemical capacitors[J]. Journal of the Electrochemical Society, 1997, 144 (4): L61-L64.

[15] Li H, Wang J, Chu Q, et al. Theoretical and experimental specific capacitance of polyaniline in sulfuric acid [J]. Journal of Power Sources, 2009, 190(2): 578-586.

[16] Zhu M, Huang Y, Huang Y, et al. A highly durable, transferable, and substrate-versatile high-performance all-polymer micro-supercapacitor with plug-and-play function[J]. Advanced Materials, 2017, 29(16): 1605137.

[17] Shen C, Wang C P, Sanghadasa M et al. Flexible micro-supercapacitors prepared using direct-write nanofibers[J]. RSC Advances, 2017, 7(19): 11724-11731.

[18] Wang X, Xu M, Fu Y et al. A highly conductive and hierarchical PANI micro/nanostructure and its supercapacitor application[J]. Electrochimica Acta, 2016, 222: 701-708.

[19] Zhao Z, Xie Y. Enhanced electrochemical performance of carbon quantum dots-polyaniline hybrid [J]. Journal of Power Sources, 2017, 337: 54-64.

[20] Itoi H, Hayashi S, Matsufusa H et al. Electrochemical synthesis of polyaniline in the micropores of activated carbon for high-performance electrochemical capacitors[J]. Chemical Communications, 2017, 53(22): 3201-3204.

[21] Chen G Z, Shaffer M S P, Coleby D, et al. Carbon nanotube and polypyrrole composites: Coating and doping[J]. Advanced Materials, 2000, 12(7): 522-526.

[22] Hughes M, Chen G Z, Shaffer M S P et al. Electrochemical capacitance of a nanoporous composite of carbon nanotubes and polypyrrole[J]. Chemistry of Materials, 2002, 14(4): 1610-1613.

[23] Hughes M, Shaffer M S P, Renouf A C, et al. Electro-

chemical capacitance of nanocomposite films formed by coating aligned arrays of carbon nanotubes with polypyrrole[J]. Advanced Materials, 2002, 14(5): 382-385.

[24] Snook G A, Chen G Z, Fray D J, et al. Studies of deposition of and charge storage in polypyrrole-chloride and polypyrrole-carbon nanotube composites with an electrochemical quartz crystal microbalance[J]. Journal of Electroanalytical Chemistry, 2004, 568(1/2): 135-142.

[25] Wu M Q, Snook G A, Gupta V, et al. Electrochemical fabrication and capacitance of composite films of carbon nanotubes and polyaniline[J]. Journal of Materials Chemistry, 2005, 15(23): 2297-2303.

[26] Peng C, Snook G A, Fray D J, et al. Carbon nanotube stabilised emulsions for electrochemical synthesis of porous nanocomposite coatings of poly 3,4-ethylene-dioxythiophene[J]. Chemical Communications, 2006, (44): 4629-4631.

[27] Snook G A, Peng C, Fray D J, et al. Achieving high electrode specific capacitance with materials of low mass specific capacitance: Potentiostatically grown thick micro-nanoporous PEDOT films[J]. Electrochemistry Communications, 2007, 9(1): 83-88.

[28] Snook G A, Chen G Z. The measurement of specific capacitances of conducting polymers using the quartz crystal microbalance[J]. Journal of Electroanalytical Chemistry, 2008, 612(1): 140-146.

[29] Peng C, Jin J, Chen G Z. A comparative study on electrochemical co-deposition and capacitance of composite films of conducting polymers and carbon nanotubes[J]. Electrochimica Acta, 2007, 53(2): 525-537.

[30] Peng C, Zhang S W, Zhou X H, et al. Unequalisation of electrode capacitances for enhanced energy capacity in asymmetrical supercapacitors[J]. Energy & Environmental Science, 2010, 3(10): 1499-1502.

[31] Zhou X H, Peng C, Chen G Z. 20 V stack of aqueous supercapacitors with carbon (-), titanium bipolar plates and CNT-polypyrrole composite (+)[J]. Aiche Journal, 2012, 58(3): 974-983.

[32] Zhou X, Chen G Z. Electrochemical performance of screen-
printed composite coatings of conducting polymers and carbon nanotubes on titanium bipolar plates in aqueous asymmetrical supercapacitors[J]. Journal of Electrochemistry, 2012, 18(6): 548-565.

[33] Cherusseri J, Kar K K. Polypyrrole-decorated 2D carbon nanosheet electrodes for supercapacitors with high areal capacitance[J]. RSC Advances, 2016, 6(65): 60454-60466.

[34] Wang H W, Zhang Y, Sun W P, et al. Conversion of uniform graphene oxide/polypyrrole composites into functionalized 3D carbon nanosheet frameworks with superior supercapacitive and sodium-ion storage properties[J]. Journal of Power Sources, 2016, 307: 17-24.

[35] Bleda-Martinez M J, Peng C, Zhang S G, et al. Electrochemical methods to enhance the capacitance in activated carbon/polyaniline composites[J]. Journal of the Electrochemical Society, 2008, 155(9): A672-A678.

[36] Jian X, Li J G, Yang H M, et al. Carbon quantum dots reinforced polypyrrole nanowire via electrostatic self-assembly strategy for high-performance supercapacitors[J]. Carbon, 2017, 114: 533-543.

[37] Dai Z X, Peng C, Chae J H, et al. Cell voltage versus electrode potential range in aqueous supercapacitors[J]. Scientific Reports, 2015, 5: 9854.

[38] Trasatti S, Buzzanca G. Ruthenium dioxide: A new interesting electrode material. Solid state structure and electrochemical behaviour[J]. Journal of Electroanalytical Chemistry and Interfacial Electrochemistry, 1971, 29(2): A1-A5.

[39] Zheng J P, Cygan P J, Jow T R. Hydrous ruthenium oxide as an electrode material for electrochemical capacitors[J]. Journal of the Electrochemical Society, 1995, 142 (8): 2699-2703.

[40] Zheng J P. Ruthenium oxide-carbon composite electrodes for electrochemical capacitors[J]. Electrochemical and Solid State Letters, 1999, 2(8): 359-361.

[41] Pang S C, Anderson M A, Chapman T W. Novel electrode materials for thin-film ultracapacitors: Comparison of electrochemical properties of sol-gel-derived and electrodeposited manganese dioxide[J]. Journal of the Electrochemical Society, 2000, 147(2): 444-450.

[42] Wu M Q, Snook G A, Chen G Z, et al. Redox deposition of manganese oxide on graphite for supercapacitors[J]. Electrochemistry Communications, 2004, 6(5): 499-504.

[43] Jin X, Zhou W, Zhang S, et al. Nanoscale microelectrochemical cells on carbon nanotubes[J]. Small, 2007, 3(9): 1513-1517.

[44] Ng KC, Zhang S W, Peng C, et al. Individual and bipolarly stacked asymmetrical aqueous supercapacitors of CNTs/SnO_2 and CNTs/MnO_2 nanocomposites[J]. Journal of the Electrochemical Society, 2009, 156(11): A846-A853.

[45] Zhang S W, Peng C, Ng K C, et al. Nanocomposites of manganese oxides and carbon nanotubes for aqueous supercapacitor stacks[J]. Electrochimica Acta, 2010, 55(25): 7447-7453.

[46] Liu Z N, Xu K L, Sun H, et al. One-step synthesis of single-layer MnO_2 nanosheets with multi-role sodium dodecyl sulfate for high-performance pseudocapacitors [J].

Small, 2015, 11(18): 2182-2191.

[47] Zhang F, Zhang T F, Yang X, et al. A high-performance supercapacitor-battery hybrid energy storage device based on graphene-enhanced electrode materials with ultrahigh energy density[J]. Energy & Environmental Science, 2013, 6(5): 1623-1632.

[48] Chae J H, Chen G Z. 1.9 V aqueous carbon-carbon supercapacitors with unequal electrode capacitances[J]. Electrochimica Acta, 2012, 86: 248-254.

[49] Bichat M P, Raymundo-Piñero E, Béguin F. High voltage supercapacitor built with seaweed carbons in neutral aqueous electrolyte[J]. Carbon, 2010, 48(15): 4351-4361.

[50] Demarconnay L, Raymundo-Piñero E, Béguin F. A symmetric carbon/carbon supercapacitor operating at 1.6 V by using a neutral aqueous solution[J]. Electrochemistry Communications, 2010, 12(10): 1275-1278.

[51] Gromadskyi D G, Chae J H, Norman S A, et al. Correlation of energy storage performance of supercapacitor with iso-propanol improved wettability of aqueous electrolyte on activated carbon electrodes of various apparent densities[J]. Applied Energy, 2015, 159: 39-50.

[52] Makino S, Shinohara Y, Ban T, et al. 4 V class aqueous hybrid electrochemical capacitor with battery-like capacity[J]. RSC Advances, 2012, 2(32): 12144-12147.

提高电容性电化学储能装置能量容量的一些尝试

余林颇[1]，陈　政[1,2,*]

(1. 宁波诺丁汉大学，理工学院化学与环境工程及可持续能源技术研究中心，宁波 315100；
2. 诺丁汉大学，工程学部化学与环境工程系，英国，诺丁汉 NG7 2RD)

摘要：本文从作者所在的课题组在超级电容器和超级电容电池方向的研究内容为基础，在电极材料和装置层面综述了电容性电化学储能装置的发展. 导电聚合物和过渡金属氧化物分别与碳纳米管复合后的复合物能显著提高前两者作为电容性法拉第储能电极的电容性能. 活性碳和碳黑等一类碳材料则可作为非法拉第储能的电极材料. 通过对超级电容器正负极电容做相应的匹配调整可以提高超级电容器的最大充电电压，从而提高超级电容器的能量容量. 此外，为了与实际设备相匹配，超级电容可以以双极板的方式串联堆积，满足高电压的需求. 超级电容电池作为新一代的电容性电化学储能装置，分别由具有电容性和法拉第电荷储存原理的电极组成，具有高比功率和高比能量的特点，也是近年来的研究热点.

关键词：超级电容器；超级电容池；赝电容；碳纳米管；活性碳